International Journal of Modern Physics E
Vol. 21, No. 10 (2012) 1250086 (13 pages)

DOI: 10.1142/S0218301312500863

World Scientific
www.worldscientific.com

DETECTION OF NEUTRINOS FROM MICRO-QUASARS II

MERCEDES ELISA MOSQUERA
Facultad de Ciencias Astronómicas y Geofísicas, Universidad Nacional de La Plata, Paseo del Bosque, (1900) La Plata, Argentina
mmosquera@fcaglp.unlp.edu.ar

OSVALDO CIVITARESE*
Department of Physics, University of La Plata, 49 y 115. c.c. 67 (1900), La Plata, Argentina
osvaldo.civitarese@fisica.unlp.edu.ar

Received 14 February 2012
Revised 10 September 2012
Accepted 11 September 2012
Published 12 October 2012

Considering a system composed of a compact object and a star subrounded by wind, and using models for high-energy proton emission from micro-quasars, we calculate the neutrino flux resulting from proton–proton collisions, with and without including neutrino oscillations. It is found that the flux of neutrinos from a windy micro-quasar is affected by neutrino oscillations, and that it reflects upon the increase in the time of observation, by a factor of the order 2–3.

Keywords: Cosmic says; astronomical observation; windy quasars; neutrino oscillations.

PACS Number(s): 95.85.Ry, 98.54.Aj, 14.60.Pq

1. Introduction

Micro-quasars are capable of accelerating particles to very high energy,[1] and they are a source of high-energy neutrinos. The matter content of the micro-quasar's jets is still unknown; however, since the jets are a source of high-energy neutrinos, they should have relativistic hadrons and radiation or matter fields that provide target protons.[2] In Ref. 3 the target protons were provided by the spherically symmetric stellar wind of the companion.

Neutrino oscillations are crucial in neutrino physics.[4–16] The impact of neutrino oscillations on highly energetic neutrinos, like those expected from the supernova

*Corresponding author.

remnant RX J1713.7-3946 (1–200 TeV neutrinos), has been studied in Ref. 17. Therein, the effect of neutrino-oscillations upon the spectrum and on the cumulative probability distribution of muons and anti-muons was found to be very important. In Ref. 15 the effect of neutrino oscillations upon neutrinos generated by *pp* interactions has been calculated as a function of the ratio between the distance to the source and the energy of the neutrinos. The authors of Ref. 15 have shown that the initial neutrino-flavor ratios are indeed very much affected by neutrino oscillations, and they have suggested a criterion, based on the distance to energy ratio, to estimate the expected flavor composition of the detected neutrinos.

In the present work, we include in the formalism the effects of the stellar wind of the companion star, and we calculate neutrino-signals from the system, to be expected to occur in a km-scale detector, such as IceCube.[18] The neutrinos are produced in a micro-quasar jet, from the interaction of relativistic protons of the jet with the proton targets of the stellar wind of the companion star. We perform this calculation considering neutrino oscillations. We compare the neutrino flux, with and without neutrino oscillations, with the sensitivity of a km-scale neutrino detector.[19,20]

This work is organized as follows. In Sec. 2, we discuss the high-energy model and the formalism needed to calculate the neutrino flux. We present and discuss the results in Sec. 3. The conclusions are drawn in Sec. 4.

2. Formalism

We consider a binary system formed by one high-mass primary star of type $B0$, with mass $M_\star = 30M_\odot$, subrounded by a disk and a compact object of mass $M_{\rm co} = 5M_\odot$, which describes a Kepler-orbit with a period of 30 days. The compact object ejects a relativistic jet, with electrons and protons, perpendicular to the accretion-disk plane, which is coincident with the orbital plane. This jet extends over 400 AU. The distance to the system is approximately equal to 2 kpc (distance from the Sun). Their relative position is written as

$$r(\psi) = \frac{a(1-e^2)}{1-e\cos(\psi)}, \tag{1}$$

where e is the eccentricity (for this system: $e = 0.7$), a is the semi-mayor axis of the ellipse, calculated from Kepler Law, and ψ is the orbital phase. For the description of the wind velocity of the stellar disk, of the primary star, we use the model proposed in Ref. 3, that is

$$v(r_w) = v_\infty \left(1 - \frac{R_\star}{r_w}\right)^\beta, \tag{2}$$

where r_w is the radial coordinate from the center of the star (it is a function of ψ and z), $R_\star = 10\ R_\odot$ is the star radius, $\beta \approx 1$ and $v_\infty = 2500$ km s^{-1} is the terminal velocity of the wind. The mass density of the wind is obtained from the

continuity equation

$$\rho_w(r_w) = \frac{\dot{M}_\star}{4\pi v_\infty r_w^2}\left(1 - \frac{R_\star}{r_w}\right)^{-\beta}, \tag{3}$$

where $\dot{M}_\star$ is the mass losing rate ($5 \times 10^{-5} M_\odot$ yr^{-1}).

We consider that the jet axis is perpendicular to the orbital plane, and that it can be represented by a cone with radius $R(z) = R_0 \frac{z}{z_0}$, with $z_0 = 10^5$ m and $R_0 = 10^4$ m.

The proton spectrum, in the jet frame, can be written as[3]

$$N'_p(E'_p) = K_p {E'_p}^{-2.2}, \tag{4}$$

where K_p is a normalization constant. The accretion rate is

$$Q_j(\psi, z) = f_{\rm acc}\dot{M}_c(\psi, z)c^2, \tag{5}$$

where $f_{\rm acc} = 0.01$ and $\dot{M}_c$ is the mass accretion rate of the compact object due to the wind,[2]

$$\dot{M}_c(\psi, z) = \frac{4\pi (G M_{\rm co})^2 \rho_w(\psi, z)}{v_{\rm rel}^3(\psi, z)}\,. \tag{6}$$

In the above expression, $v_{\rm rel}$ is the velocity relative to the circumstellar wind.[21]

The proton flux, in the observer frame, is

$$J_p(\psi, E_p, z, \theta) = \frac{c}{4\pi} K_p(\psi)\left(\frac{z_0}{z}\right)^2 \Gamma^{1-\alpha} \times \frac{(E_p - \beta_p \epsilon\cos\theta)^{-\alpha}}{\left[\sin^2\theta + \Gamma^2\left(\cos\theta - \dfrac{E_p\beta_p}{\epsilon}\right)^2\right]^{1/2}}, \tag{7}$$

where $\epsilon = \sqrt{E_p^2 - M_p^2 c^4}$, $\alpha = 2.2$, $\Gamma = 1.25$ is the Lorentz factor, $\beta_b = \Gamma^{-1}\sqrt{\Gamma^2 - 1}$ and θ is the viewing angle (see Ref. 3 for details). These protons interact with target protons of the wind *via* the reaction

$$p + p \to p + p + \xi_{\pi^0}(E_P)\pi^0 + \xi_\pi(E_P)(\pi^+ + \pi^-)\,, \tag{8}$$

where $\xi_{\pi^0}(E_P)$ and $\xi_\pi(E_P)$ are the multiplicities for neutral and charged pions, respectively (as defined below). The charged pions decay into muons and produce gamma-rays and neutrinos that can travel almost freely. This gamma-ray emissivity can be written as[22]

$$q_\gamma(\psi, E_\gamma, z, \theta) = 4\pi\eta_A\sigma_{pp}(E_p)\frac{2Z^{(\alpha)}_{p\to\pi^0}}{\alpha}J_p(\psi, E_\gamma, z, \theta)\,,$$

where $\eta_A = 1.4$ and $Z^{(\alpha)}_{p\to\pi^0} = 0.092$ is the spectrum-weighted moment of the inclusive cross-section.[23] The cross-section for pp reactions is, in units of m^2,

$$\sigma_{pp}(E) = 30\left(0.95 + 0.06\log\left(\frac{E}{10^3\ {\rm MeV}}\right)\right) \times 10^{-31}.$$

According to Ref. 2, the proton (E_p) and photon (E_γ) energies are related by $E_p = 6k^{-1}\xi_{\pi^0}(E_p)E_\gamma$, where $k = 0.5$ is the inelasticity coefficient and $\xi_{\pi^0}(E_p) = 1.1(\frac{E_p}{10^3\ \mathrm{MeV}})^{1/4}$.

The neutrino intensity, produced by pion- and muon-decay, and the spectral flux are related by energy conservation[24,25]:

$$\int_{E_\gamma^{\min}}^{E_\gamma^{\max}} \mathrm{d}E_\gamma \frac{\mathrm{d}N_\gamma}{\mathrm{d}E_\gamma} E_\gamma = \Delta \int_{E_\nu^{\min}}^{E_\nu^{\max}} \mathrm{d}E_\nu \frac{\mathrm{d}N_\nu}{\mathrm{d}E_\nu} E_\nu \,, \tag{9}$$

where $E_\gamma^{\min}$ and $E_\gamma^{\max}$ are the minimum and maximum energies of photons resulting from hadrons, and $E_\nu^{\min}$ and $E_\nu^{\max}$ are the corresponding minimum and maximum energy of the neutrinos. The factor Δ depends on the channel (pp channel or $p\gamma$ channel), in this case $\Delta = 1$.[25] The neutrino energy is related to the photon energy by $E_\nu = \frac{1}{2}E_\gamma$, and the photon energy is related to the energy of accelerated protons $E_p = 6E_\gamma$. However, if we consider the multiplicities ξ_π, for inelastic proton–proton interactions, the gamma-ray energy can be written as[26]

$$E_p = \frac{6}{k}\xi_\pi(E_p)E_\gamma, \tag{10}$$

where

$$\xi_\pi(E_p) = \left(\frac{E_p}{10^3\ \mathrm{MeV}} - 1.22\right)^{1/5}. \tag{11}$$

Finally, the neutrino energy can be obtained from the proton energy as

$$E_\nu = \frac{k}{12\xi_\pi(E_p)} E_p \,. \tag{12}$$

The maximum neutrino energy is determined by the maximum energy acquired by the accelerated protons, which is related to the magnetic field B. The magnetic field is calculated by assuming equipartition between the magnetic field energy and the kinetic energy of the jet,[2] leading to the following expression:

$$B(\psi, z) = \sqrt{\frac{8 f_{\mathrm{em}} \dot{M}_c(\psi, z)}{R^2(z) v_j m_p} E_k} \,, \tag{13}$$

where E_k is the mean cold proton kinetic energy, $v_j = \beta_b c$ and $f_{\mathrm{em}} = 0.1$ is the fraction of ejected matter of the accreted matter $\dot{M}_c$. The maximum energy of the protons is

$$E_p(\psi) = eR(z_0)B(\psi, z_0) \,. \tag{14}$$

Thus, the muon-neutrino intensity can be obtained by performing the integrals[2]

$$I_\nu(E_\nu, \psi, \theta) = 4 \int \mathrm{d}V \frac{f_p}{m_p} \rho_w(r_w) q_\gamma(\psi, 2E_\nu, z, \theta) \,, \tag{15}$$

where $f_p = 0.1$ takes into account particle-rejection from the boundary.[27] The electron–neutrino intensity can be determined by repeating the same arguments.

2.1. *Vacuum neutrino oscillations*

The light neutrino mass eigenstates $|\nu_1\rangle$, $|\nu_2\rangle$, $|\nu_3\rangle$, and neutrino flavor states $|\nu_e\rangle$, $|\nu_\mu\rangle$, $|\nu_\tau\rangle$, are related by the mixing matrix U. If we considered the approximation $\theta_{13} \simeq 0$,[a] the matrix takes the form[29]

$$U = \begin{pmatrix} c_{12} & s_{12} & 0 \\ -s_{12}c_{23} & c_{23}c_{12} & s_{23} \\ s_{23}s_{12} & -s_{23}c_{12} & c_{23} \end{pmatrix} . \tag{16}$$

In this notation, $c_{ij}(s_{ij})$ represents $\cos\theta_{ij}$ $(\sin\theta_{ij})$, where θ_{ij} is the mixing angle between the mass eigenstates i and j.

If the difference between the neutrino mass eigenstates does not vanish, the probability $P_{\alpha\beta} = |\langle\nu_\alpha(t)|\nu_\beta\rangle|^2$, which is the probability of detecting a ν_α-type neutrino when a ν_β-type neutrino was emitted, is not null. The survival and conversion probabilities can be written as

$$\begin{aligned}
P_{\text{vac}}^{\nu_\mu\nu_\mu}(E_\nu) &= 1 - \sin^2 2\theta_{12}\cos^4\theta_{23}\sin^2\left(\frac{\Delta m_{12}^2 c^4 d}{4E_\nu\hbar c}\right) \\
&\quad - \sin^2\theta_{12}\sin^2 2\theta_{23}\sin^2\left(\frac{\Delta m_{13}^2 c^4 d}{4E_\nu\hbar c}\right) \\
&\quad - \cos^2\theta_{12}\sin^2 2\theta_{23}\sin^2\left(\frac{\Delta m_{23}^2 c^4 d}{4E_\nu\hbar c}\right) , \\
P_{\text{vac}}^{\nu_\mu\nu_e}(E_\nu) &= \cos^2\theta_{23}\sin^2 2\theta_{12}\sin^2\left(\frac{\Delta m_{12}^2 c^4 d}{4E_\nu\hbar c}\right) , \\
P_{\text{vac}}^{\nu_\mu\nu_\tau}(E_\nu) &= -\frac{1}{4}\sin^2 2\theta_{12}\sin^2 2\theta_{23}\sin^2\left(\frac{\Delta m_{12}^2 c^4 d}{4E_\nu\hbar c}\right) \\
&\quad + \sin^2\theta_{12}\sin^2 2\theta_{23}\sin^2\left(\frac{\Delta m_{13}^2 c^4 d}{4E_\nu\hbar c}\right) \\
&\quad + \cos^2\theta_{12}\sin^2 2\theta_{23}\sin^2\left(\frac{\Delta m_{23}^2 c^4 d}{4E_\nu\hbar c}\right) , \\
P_{\text{vac}}^{\nu_\tau\nu_e}(E_\nu) &= \sin^2\theta_{23}\sin^2 2\theta_{12}\sin^2\left(\frac{\Delta m_{12}^2 c^4 d}{4E_\nu\hbar c}\right) , \\
P_{\text{vac}}^{\nu_e\nu_e}(E_\nu) &= 1 - \sin^2 2\theta_{12}\sin^2\left(\frac{\Delta m_{12}^2 c^4 d}{4E_\nu\hbar c}\right) ,
\end{aligned} \tag{17}$$

where $\Delta m_{ij}^2 = m_i^2 - m_j^2$ are the square-mass differences between the masses of neutrino-mass eigenstates m_i and m_j, E_ν is the neutrino energy and d is the distance between the source and the detectors.

[a]For simplicity, we have taken $\theta_{13} \simeq 0$, although more recent estimations of θ_{13} could be consistent with $\theta_{13} \neq 0$.[28]

Experiments with solar, atmospheric and reactor neutrinos have provided strong evidences on the neutrino oscillations, and the analysis of the data has determined the neutrino oscillation parameters.[4,6–8,10,30,31] For three flavors we adopt the best fit parameters obtained by[32–34]

$$\begin{aligned} \Delta m^2_{12} &= 7.65 \times 10^{-5}\ \mathrm{eV}^2\,, \\ \sin^2\theta_{12} &= 0.304\,, \\ \Delta m^2_{31} &\simeq \Delta m^2_{32} = 2.40 \times 10^{-3}\ \mathrm{eV}^2\,, \\ \sin^2\theta_{23} &= 0.5\,. \end{aligned} \tag{18}$$

2.2. *Neutrino oscillations in matter*

When a neutrino travels across the Earth, the electrons might interact with it (MSW effect[35,36]). In order to obtain the survival probability (or the conversion probability) of any neutrino, in the evolution equation of the neutrino states, one must incorporate a matter-induced neutrino potential V,[37]

$$\imath\frac{\mathrm{d}\nu_f}{\mathrm{d}t} = \left(\frac{UM^2U^\dagger}{2E} + V\right)\nu_f\,, \tag{19}$$

where $M^2 = \mathrm{diag}(0, \Delta m^2_{12}, \Delta m^2_{13})$, $V = \mathrm{diag}(V_e, 0, 0)$, $V_e = \sqrt{2}G_F N_e(r)$, G_F is the Fermi constant and $N_e(r)$ is the Earth electron density.

Following Peres and Smirnov,[37] one can perform a rotation in θ_{23} in order to work in the base $\tilde{\nu} = (\nu_e, \tilde{\nu}_2, \tilde{\nu}_3)$. In this case, the $\tilde{\nu}_3$-state decouples from the rest of the system and evolves independently, and thus the evolution matrix $S = U_{23}\tilde{S}U^\dagger_{23}$ decouples. The survival and conversion probabilities can be calculated as[37]

$$\begin{aligned} P^{\nu_e\nu_e}_{\oplus} &= 1 - P_2\,, \\ P^{\nu_e\nu_\mu}_{\oplus} &= \cos^2\theta_{23}P_2\,, \\ P^{\nu_e\nu_\tau}_{\oplus} &= \sin^2\theta_{23}P_2\,, \\ P^{\nu_\tau\nu_\mu}_{\oplus} &= \frac{1}{2}\sin^2 2\theta_{23}\left(1 - \frac{1}{2}P_2 - \sqrt{1-P_2}\cos\phi\right), \\ P^{\nu_\mu\nu_\mu}_{\oplus} &= 1 - \cos^4\theta_{23}P_2 \\ &\quad - \frac{1}{2}\sin^2 2\theta_{23}\Big(1 - \sqrt{1-P_2}\cos\phi\Big)\,, \end{aligned} \tag{20}$$

where $\phi = \phi_3 - \phi_2$, $\phi_3 = \frac{\Delta m^2_{13}}{2E}L$, L is the total lenght of the neutrino trajectory inside the Earth and $P_2 = |A_{e2}|^2$. In order to obtain P_2, one can now work in the basis $\tilde{\nu} = (\nu_e, \tilde{\nu}_2)$. Following Ref. 38 we obtain the eigenvalues of the new Hamiltonian (in the new two-state basis) and perform the decomposition

$H = H_0 + H_1$, where

$$H_0 = \omega \begin{pmatrix} 1 & 0 \\ 0 & -1 \end{pmatrix}, \tag{21}$$

$$H_1 = \sin 2\theta_{12} \frac{\Delta m_{12}^2}{4E} \begin{pmatrix} -\epsilon & 1 \\ 1 & \epsilon \end{pmatrix} \tag{22}$$

and

$$\omega = \sqrt{\left(\frac{V_e}{2} - \frac{\Delta m_{12}^2}{4E} \cos 2\theta_{12}\right)^2 + \left(\frac{\Delta m_{12}^2}{4E}\right)^2 \sin^2 2\theta_{12}},$$

$$\epsilon = \frac{\cos 2\theta_{12} \frac{\Delta m_{12}^2}{4E} + \omega - \frac{V_e}{2}}{\sin 2\theta_{12} \frac{\Delta m_{12}^2}{4E}}. \tag{23}$$

Performing the same approximations of Ref. 38, we take H_1 as a small perturbation and decompose the amplitude matrix as $S = S_0 S_1$, where $\imath \frac{\mathrm{d}S_0}{\mathrm{d}x} = H_0 S_0$ and $\imath \frac{\mathrm{d}S_1}{\mathrm{d}x} \approx S_0^{-1} H_0 S_0$. Finally,

$$P_2 = \sin^2 2\theta_{12} \left(\frac{\Delta m_{12}^2}{4E}\right)^2 \left| \int_0^L \mathrm{d}y \, e^{-\imath 2\psi(y)} \right|^2,$$

with $\psi(x) = \int_0^x \mathrm{d}y \, \omega(y)$.

The matter distribution on the Earth is symmetric with respect to the middle point of the neutrino trajectory, and so the last integral can be written as[38]

$$P_2 = 4 \frac{\sin^2 2\theta_{12}}{\omega(L)^2} \left(\frac{\Delta m_{12}^2}{4E}\right)^2 \times \left(\sin \psi_L + \omega(L) \int_0^{L/2} \mathrm{d}y \frac{\sin 2\psi(y)}{\omega(y)^2} \frac{\mathrm{d}\omega(y)}{\mathrm{d}y}\right)^2,$$

where $\psi_L = \psi(L)$.

In order to obtain the neutrino oscillation probability, we use the parametrization of the Earth matter density presented in Ref. 39, that is

$$N_j(x) = \alpha_j' + \beta_j' x^2 + \gamma_j' x^4, \tag{24}$$

for nonradial trajectories, where x is the trajectory coordinate and the sub-index j represent the shell (there are five of these shells in the model of Ref. 39).

The total longitude of the neutrino trajectory, L, depends on the nadir angle, η, of the observatory as $L = 2R_\oplus \cos\eta$. The neutrino can go through different shells, depending of the nadir angle, and the trajectory coordinate in each shell also depends on the nadir angle since $x_j = R_\oplus \sqrt{r_j^2 - \sin^2 \eta}$ (obviously, if $\eta > \frac{\pi}{2}$ the neutrino does not enter the Earth).

Because the potential changes slowly with the distance, the second term in Eq. (24) can be neglected, except when the neutrino crosses between two shells.[38] In this case

$$P_2 = 4\frac{\sin^2 2\theta_{12}}{\omega(L)^2}\left(\frac{\Delta m^2_{12}}{4E}\right)^2\left(\sin\psi_L - \omega(L)\sum_{i=1}^{4}\frac{\omega(x_i^+)-\omega(x_i^-)}{\omega(x_i^-)\omega(x_i^+)}\sin 2\psi_i\right)^2, \quad (25)$$

where x_i represents the value of the radii of the spherical shell i, $\omega(x_i^+)$ and $\omega(x_i^-)$ are the right and left limit of $\omega(x)$, respectively, and $\psi_i = \psi(x_i)$.

2.3. *Vacuum neutrino oscillation and matter effects*

The muon-neutrino survival probability can be obtained as[40]

$$P_{\rm osc}^{\nu_\mu\nu_\mu} = \sum_\gamma P_\oplus^{\nu_\mu\nu_\gamma} P_{\rm vac}^{\nu_\gamma\nu_\mu}\,. \quad (26)$$

Meanwhile, the conversion between electron-neutrinos and muon-neutrinos is

$$P_{\rm osc}^{\nu_e\nu_\mu} = \sum_\gamma P_\oplus^{\nu_e\nu_\gamma} P_{\rm vac}^{\nu_\gamma\nu_\mu}\,. \quad (27)$$

2.4. *Neutrino detection*

In a micro-quasar jet, muon- and electron-neutrinos are produced, but only the muon-neutrinos can be detected by an IceCube[18] type detector. In the previous sections we have calculated the neutrino intensity, which is needed to estimate signals of muon-neutrinos at energies of about 1–10^3 TeV. This function I_ν [of Eq. (15)] should be integrated with the probability that a neutrino of energy $E_\nu \sim 1$–10^3 TeV on a trajectory to the detector produces a muon-neutrino[41]:

$$P(E) = 1.3\times 10^{-6}\left(\frac{E}{10^6\ \text{MeV}}\right)^{0.8}. \quad (28)$$

Therefore, the signal can be written as

$$S_\nu(\theta) = \frac{T_{\rm obs}A_{\rm eff}}{4\pi d^2}\int_0^{2\pi}{\rm d}\psi\int_{10^6\ \text{MeV}}^{E_\nu^{\rm max}} I_\nu(E,\psi,\theta)P(E){\rm d}E\,, \quad (29)$$

where $T_{\rm obs}$ is the observational period of time and $A_{\rm eff} = 10^6$ m^2 is the effective area of the detector. If we consider neutrino oscillations, the function $I_\nu(E,\psi,\theta)$ can be written as $I_\nu(E,\psi,\theta) = I_{\nu_\mu}(E,\psi,\theta)P_{\rm osc}^{\nu_\mu\nu_\mu}(E) + I_{\nu_e}(E,\psi,\theta)P_{\rm osc}^{\nu_e\nu_\mu}(E)$.

The noise above 1 TeV can be written as[2]

$$N = \sqrt{T_{\rm obs}A_{\rm eff}\Delta\Omega\int_{10^6\ \text{MeV}}^{E_\nu^{\rm max}} F_B(E)P(E){\rm d}E}\,, \quad (30)$$

where

$$F_B(E) = 2\left(\frac{E}{10^3\ \text{MeV}}\right)^{-3.21}\ \text{MeV}^{-1}\text{m}^{-2}\text{s}^{-1}\text{sr}^{-1}$$

is the flux of atmospheric neutrinos.[42] We take the value $\Delta\Omega = 3\times 10^{-4}$ sr for the solid angle of the search bin.

3. Results

We have performed the calculation of the neutrino signal on a km-scale detector, for a parametrization of the wind mass density and velocity (see Sec. 2) and for different values of the viewing angle θ. We have computed the signal-to-noise ratio Ω ($\Omega = S_\nu/N$) considering neutrino oscillations ($\Omega_{\rm osc}$) and without considering neutrino oscillations (Ω). We have assumed one year of observational time. The noise values are of the order of 2. We present our results in Fig. 1. As one can expect, the greatest the viewing angle, the lower is the neutrino signal.

The observational time, from Eqs. (29) and (30), is given by

$$\Omega(T) = T^{1/2}\Omega \quad (T = 1 \text{ year})\,. \tag{31}$$

As shown by the curves of Fig. 1, the signal-to-noise ratio depends strongly on the neutrino oscillations. Without ν-oscillations, and for $\theta_{\rm obs} < 50^\circ$, the signal-to-noise ratio Ω varies between 3 and 12, and the corresponding observational time is of the order of 1 year. However, if neutrino oscillations are considered in the calculations, $\Omega_{\rm osc}$ varies between 3 and 6 for an observational angle smaller than 30°. If this is the case, the time of observation would be approximately 2 years for $\theta_{\rm obs} \approx 30^\circ$ and 5 years for $\theta_{\rm obs} \approx 45^\circ$. The effects due to the Earth matter upon the neutrino oscillations depend on the nadir angle but they are small effects, indeed, as we have seen from our results.

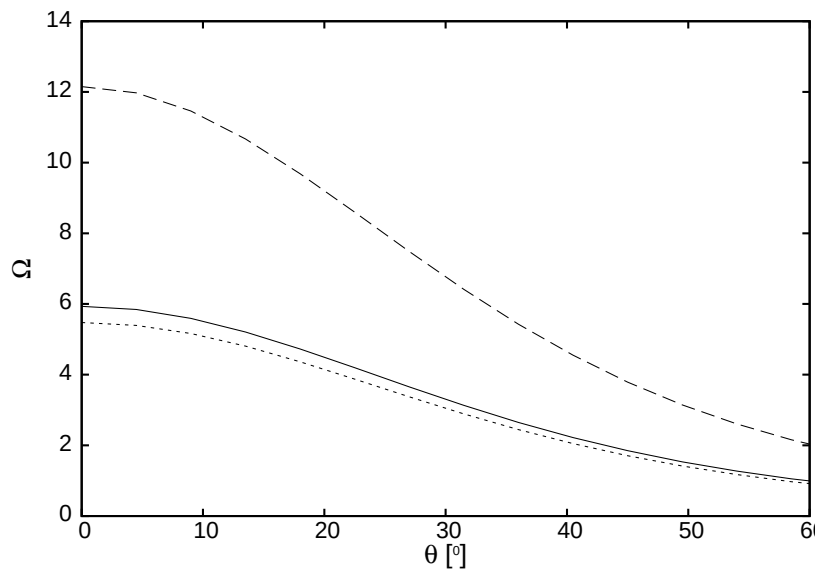

Fig. 1. Neutrino signal-to-noise ratio as a function of the viewing angle θ. The ratio Ω, calculated without including neutrino oscillations is shown by the long-dashed line. The results for $\Omega_{\rm osc}$, obtained by considering only vacuum neutrino oscillation are represented by the solid line. The dotted line corresponds to the results obtained by including neutrino oscillations, in the presence of both vacuum and matter effects. The nadir angle is $\eta = 30^\circ$.

For completeness we have studied the dependence of the ratio Ω as function of the following parameters: the terminal velocity of the wind, the mass losing rate of the wind and the Lorentz factor while the viewing angle remains constant at $\theta_{\rm obs} = 30°$. If we increase the terminal velocity of the wind or if we decrease the mass losing rate of the wind, the mass density of the wind decreases, resulting in the decrease of the accretion rate of the compact object [see Eq. (6)]. Thus, a reduction of the neutrino intensity is observed (see Figs. 2 and 3).

If the terminal velocity of the wind is lower than 3×10^3 km s^{-1}, the resulting value of Ω is greater than 3 if neutrino oscillations are not accounted for. However, if neutrino oscillations are included in the calculations, v_∞ has to be lower ($v_\infty < 2.5 \times 10^3$ km s^{-1}) in order to get $\Omega_{\rm osc} > 3$. For instance, if $v_\infty = 3.5 \times 10^3$ km s^{-1}, the observational time is approximately 5 years if neutrino oscillation are not been taken into account, and 23 years otherwise.

Other effect occurs when the mass losing rate of the wind is modified. If $\dot{M}_\star > 3.2 \times 10^{-5} M_\odot$ yr^{-1}, then $\Omega > 3$; however, if neutrino oscillations are included, the value of the mass losing rate increases ($\dot{M}_\star > 4.7 \times 10^{-5} M_\odot$ yr^{-1}) in order to obtain $\Omega_{\rm osc} > 3$. For example, if $\dot{M}_\star = 2 \times 10^{-5} M_\odot$ yr^{-1}, the observational time increases from 7 to 30 years when neutrino oscillation effects are considered.

The Lorentz factor enters in the neutrino intensity through the proton flux. There exists a maximum value for the signal-to-noise ratio in $\Gamma \approx 2.6$. In this case, if $\Gamma < 7$ the signal-to-noise ratio is always greater than 3.

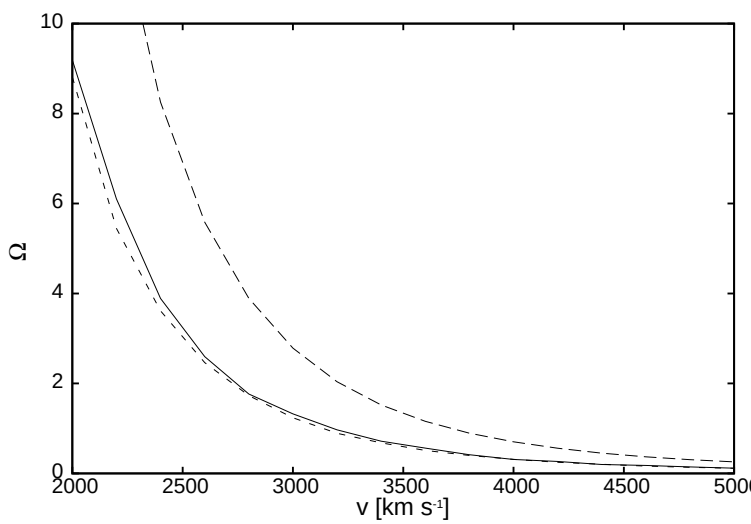

Fig. 2. Neutrino signal-to-noise ratio as a function of v_∞. The ratio Ω, calculated without including neutrino oscillations is shown by the long-dashed line. The results for $\Omega_{\rm osc}$, obtained by considering only vacuum neutrino oscillation are represented by the solid line. The dotted line corresponds to the results obtained by including neutrino oscillation, in the presence of both vacuum and matter effects. The nadir angle is $\eta = 30°$.

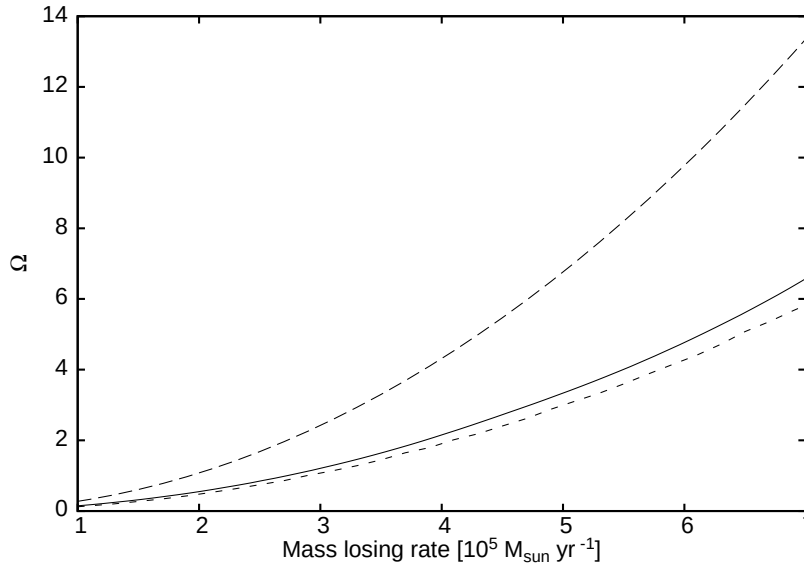

Fig. 3. Neutrino signal-to-noise ratio as a function of $\dot{M}_\star$. The ratio Ω, calculated without including neutrino oscillations is shown by the long-dashed line. The results for $\Omega_{\rm osc}$, obtained by considering only vacuum neutrino oscillation are represented by the solid line. The dotted line corresponds to the results obtained by including neutrino oscillation, in presence of both vacuum and matter effects. The nadir angle is $\eta = 30^\circ$.

For completeness we also performed the same analysis assuming $\sin^2 2\theta_{13} = 0.155$.[28] The results are similar to the previous ones (obtained considering $\theta_{13} = 0$), and their difference is less than 3%.

In all the cases studied, the signal-to-noise ratio is suppressed by neutrino oscillations. However, if the neutrinos of this kind of sources are detected in a km-scale detector, more stringent constraints on the astrophysical parameters, like the ones used in this work, can be obtained.

4. Conclusions

In the present work, we have discussed the emission of neutrinos from a system composed of a massive star, with stellar wind and a micro-quasar. In this context, the stellar wind provides target protons to the relativistic protons ejected from the micro-quasar. These interactions produce high-energy neutrinos that can be detected in a km-scale neutrino detector. We have computed the neutrino flux produced inside the jets with and without considering neutrino oscillations and as a function of the viewing angle. We found that the signal-to-noise ratio is reduced considerably by neutrino oscillations. However, in spite of this huge effect, the calculations show that it would still be possible to detect neutrinos from micro-quasar jets, over a few years-long observational time. If these neutrinos are detected,

new bounds on the astrophysical parameters that characterize micro-quasars can be established.

Acknowledgments

This work has been partially supported by the CONICET (PIP 0740) and by the ANPCYT of Argentina. The authors are members of the Scientific Research Career of the CONICET (Argentina). O.C. acknowledges with pleasure the hospitality of the Department of Physics of the University of Jyväskylä, Finland.

References

1. F. Aharonian *et al.*, *Science* **309** (2005) 746.
2. H. R. Christiansen, M. Orellana and G. E. Romero, *Phys. Rev. D* **73** (2006) 063012.
3. G. E. Romero, D. F. Torres, M. M. Kaufman and I. F. Mirabel, *Astron. Astrophys.* **410** (2003) L1.
4. The Super-Kamiokande Collab. (Y. Fukuda *et al.*), *Phys. Rev. Lett.* **81** (1998) 1562.
5. The SNO Collab. (I. Ahmad *et al.*), *Phys. Rev. Lett.* **87** (2001) 071301.
6. The SAGE Collab. (J. N. Abdurashitov *et al.*), *Phys. Rev. C* **80** (2009) 015807.
7. The Gno Collab. (M. Altmann *et al.*), *Phys. Lett. B* **616** (2005) 174.
8. The Borexino Collab. (C. Arpesella *et al.*), *Phys. Rev. Lett.* **101** (2008) 091302.
9. The KamLAND Collab. (T. Eguchi *et al.*), *Phys. Rev. Lett.* **90** (2003) 021802.
10. The K2K Collab. (M. Ahn *et al.*), *Phys. Rev. D* **74** (2006) 072003.
11. J. Bahcall, M. H. Pinsonneault and S. Basu, *Astrophys. J.* **555** (2001) 990.
12. J. Suhonen and O. Civitarese, *Phys. Rep.* **300** (1998) 123.
13. H. Ejiri, *Phys. Rep.* **338** (2000) 265.
14. C. D. Dermer and A. Atoyan, *Phys. Rev. Lett.* **91** (2003) 071102.
15. H. Athar, C. S. Kim and J. Lee, *Mod. Phys. Lett. A* **21** (2006) 1049.
16. P. Lipari, M. Lusignoli and D. Meloni, *Phys. Rev. D* **75** (2007) 123005.
17. M. L. Costantini and F. Vissani, *Astropart. Phys.* **23** (2005) 477.
18. IceCube Collab. (R. Abbasi *et al.*), *Nature* **484** (2012) 351.
19. F. Halzen, *Eur. Phys. J. C* **46** (2006) 669.
20. S. Aiello *et al.*, *Astropart. Phys.* **28** (2007) 1.
21. P. C. Gregory and C. Neish, *Astrophys. J.* **580** (2002) 1133.
22. F. A. Aharonian and A. M. Atoyan, *Astron. Astrophys.* **309** (1996) 917.
23. T. K. Gaisser, *Cosmic Rays and Particle Physics* (Cambridge University Press, 1990).
24. F. W. Stecker and M. H. Salamon, *Space Sci. Rev.* **75** (1996) 341.
25. J. Alvarez-Muñiz and F. Halzen, *Astrophys. J. Lett.* **576** (2002) 33.
26. V. L. Ginzburg and S. I. Syrovat-Skii, *Sov. Astron.* **8** (1964) 342.
27. G. E. Romero, H. R. Christiansen and M. Orellana, *Astrophys. J.* **632** (2005) 1093.
28. T2K Collab. (K. Abe *et al.*), *Phys. Rev. Lett.* **107** (2011) 041801.
29. A. Bandyopadhyay, S. Choubey, S. Goswami and K. Kar, *Phys. Rev. D* **65** (2002) 073031.
30. I. Ahmad *et al.*, *Phys. Rev. Lett.* **89** (2002) 011301.
31. T. Araki *et al.*, *Phys. Rev. Lett.* **94** (2005) 081801.
32. G. L. Fogli *et al.*, *Phys. Rev. D* **78** (2008) 033010.
33. T. Schwetz, M. A. Tortola and J. W. F. Valle, *New J. Phys.* **10** (2008) 113011.
34. M. Apollonio *et al.*, *Phys. Lett. B* **466** (1999) 415.
35. S. P. Mikheyev and A. Y. Smirnov, *Yad. Fiz.* **42** (1985) 1441.

36. L. Wolfenstein, *Phys. Rev. D* **17** (1978) 2369.
37. O. L. G. Peres and A. Y. Smirnov, *Phys. Lett. B* **456** (1999) 204.
38. E. K. Akhmedov, M. Maltoni and A. Y. Smirnov, *Phys. Rev. Lett.* **95** (2005) 211801.
39. E. Lisi and D. Montanino, *Phys. Rev. D* **56** (1997) 1792.
40. S. Razzaque and A. Y. Smirnov, *JHEP* **3** (2010) 31.
41. T. K. Gaisser, F. Halzen and T. Stanev, *Phys. Rep.* **258** (1995) 173.
42. P. Lipari, *Astropart. Phys.* **1** (1993) 399.